第 42 卷第 4 期
2023 年 8 月

红 外 与 毫 米 波 学 报
J. Infrared Millim. Waves

Vol. 42，No. 4
August，2023

文章编号：1001-9014（2023）04-0483-07 **DOI：10. 11972/j. issn. 1001-9014. 2023. 04. 009**

High-efficiency AlN/GaN MIS-HEMTs with SiN_x insulator grown in-situ for millimeter wave applications

CHEN Xiao-Juan[1,2*]， ZHANG Yi-Chuan[2]， ZHANG Shen[2]， LI Yan-Kui[2]， NIU Jie-Bin[2]， HUANG Sen[2]，
MA Xiao-Hua[1]， ZHANG Jin-Cheng[1]， WEI Ke[2*]
（1. Xidian University，Xi′an 710071，China；
2. Institute of Microelectronics，Chinese Academy of Sciences，Beijing 100029，China）

Abstract：In this work，high-efficiency AlN/GaN metal-insulator-semiconductor high electron mobility transistors（MIS-HEMTs）have been fabricated for millimeter wave applications. A 5-nm SiN_x insulator is grown in-situ as the gate insulator by metal-organic chemical vapor deposition（MOCVD），contributing to remarkably suppressed gate leakage，interface state density and current collapse. The fabricated MIS-HEMTs exhibit a maximum drain current of 2. 2 A/mm at V_{GS}=2 V，an extrinsic peak G_m of 509 mS/mm，and a reverse Schottky gate leakage current of 4. 7×10^{-6} A/mm when V_{GS} = -30 V. Based on a 0. 15 μm T-shaped gate technology，an f_T of 98 GHz and f_{MAX} of 165 GHz were obtained on the SiN/AlN/GaN MIS-HEMTs. Large signal measurement shows that，in a continuous-wave mode，the MIS-HEMTs deliver an output power density（P_{out}）of 2. 3 W/mm associated with a power-added efficiency（PAE）of 45. 2% at 40 GHz，and a P_{out}（PAE）of 5. 2 W/mm（42. 2%）when V_{DS} was further increased to 15 V.

Key words：AlN/GaN，metal-insulator-semiconductor High Electron Mobility Transistors（MIS-HEMTs），millimeter wave，low dispersion，low drain voltage

带有原位生长SiN_x绝缘层的AlN/GaN毫米波高效率MIS-HEMT器件

陈晓娟[1,2*]， 张一川[2]， 张 昇[2]， 李艳奎[2]， 牛洁斌[2]， 黄 森[2]，
马晓华[1]， 张进成[1]， 魏 珂[2*]
（1. 西安电子科技大学，陕西 西安 710071；
2. 中国科学院微电子研究所，北京 100029）

摘要：本文采用金属有机化学气相沉积(MOCVD)生长原位SiN_x栅介质制备了用于Ka波段高功率毫米波应用的AlN/GaN金属绝缘体半导体高电子迁移率晶体管(MIS-HEMTs)。原位生长SiN_x栅介质显著抑制了栅反向漏电、栅介质/AlN界面态密度和电流坍塌。所研制的MIS HEMTs在V_{GS}= 2 V时最大饱和输出电流为2.2 A/mm，峰值跨导为509 mS/mm，在V_{GS} = -30 V时肖特基栅漏电流为4.7×10^{-6} A/mm。采用0.15 μmT形栅技术，获得98 GHz的f_T和165 GHz的f_{MAX}。大信号测量表明，在连续波模式下，漏极电压V_{DS} = 8 V时，MIS HEMT在40 GHz下输出功率密度2.3 W/mm，45.2%的功率附加效率(PAE)，而当V_{DS}增加到15 V时，功率密度提升到5.2 W/mm，PAE为42.2%。

关 键 词：AlN/GaN；金属绝缘体半导体高电子迁移率晶体管；Ka波段；低损耗；低偏压

中图分类号：O48 **文献标识码**：A

Introduction

Received date：2022- 06- 22，**revised date**：2022- 11- 02 **收稿日期**：2022- 06- 22，**修回日期**：2022- 11- 02

Foundation items：Supported by the National Natural Science Foundation of China（61822407，62074161，62004213）；the National Key Research and Development Program of China under（2018YFE0125700）

Biography：CHEN Xiao-Juan（1979-），female，ChongQing，master. Research area involves Compound Semiconductor materials and devices. E-mail：chenxiaojuan@ime. ac. cn.

[*] **Corresponding authors**：E-mail：chenxiaojuan@ime. ac. cn，weike@ime. ac. cn

In recent years, high electron mobility transistors (HEMTs) based on GaN have attracted more attention, due to their high thermal conductivity, high breakdown voltage, and high-power density for millimeter-wave (mm-wave) power amplifiers. In an AlGaN/GaN HEMTs structure, the working voltage may reach 28 V or even higher[1][2], such high voltage will enhance the longitudinal electric field to increase the gate leakage[3]. Additionally, the internal electric field intensity will reach 10^6~10^7 V/cm when the 20~30 V is applied to drain bias, leading to current collapse, reduction of breakdown voltage, and increase in leakage[4]. In order to achieve high-performance GaN HEMT at low operating voltage, the energy-band theory is used to design new epitaxial structures to increase the electron gas density meanwhile preventing the gate from losing its control ability for the short T-gate. Therefore, the ultra-thin barrier layer technology has shown great advantages in ultra-high frequency and high power[5][6].

In millimeter-wave applications, the gate length is shrunk to deep-submicron size, and the transverse dimension of the device needs to be scaled down at the same proportion. To avoid the short channel effect, the material structure with an ultra-thin barrier layer is used to solve the aspect ratio of the gate. The issue primarily results from the much stronger spontaneous and piezoelectric polarization of AlN/GaN compared to AlGaN/GaN, leading to a much higher drain current in the HEMT channel, also allowing the use of a much thinner barrier layer. While along with the shrink of vertical device dimensions, increased gate leakage necessitates the use of a gate insulator[7-10].

AlN barrier has been shown highly sensitive to the air and vapor for oxidation, consequently, surface treatment and passivation techniques play a significant role in the surface state. To achieve a low gate leakage current, materials with a wide bandgap are necessary, such as SiO_2 and Al_2O_3[7][9]. However, it is inevitable that these materials are deposited on the AlN surface when it is exposed to air, becoming contamination at the interfaces. On the other hand, in-situ deposition of SiN_x is a promising way to realize proper interfaces, which guarantees the insensitivity of AlN surfaces to temperature change.

In this work, we demonstrated the AlN/ GaN MIS-HEMTs. By using in-situ SiN_x insulator, a maximum drain current $I_{D,max}$ of 2.2 A/mm was obtained at V_{GS}=2 V, it doubled $I_{D,max}$ of the AlGaN/GaN HEMTs under the same condition. Transconductance $G_{m,ext}$ of 509 mS/mm are also achieved. Moreover, the OFF-state drain leakage, as well as gate leakage current in the HEMTs, was reduced by the low interface state between AlN barrier and insulator, contributing to a low Schottky gate leakage of 4.7×10^{-6} A/mm at V_{GS} = -30 V and a low OFF-state drain leakage of 8.2×10^{-5} A/mm. Owing to the suppressed current collapse, when V_{DS} = 8 V, a high output power density of 2.3 W/mm with peak power-added-efficiency (PAE) of 45.2%, and a power gain of 10.2 dB are achieved at 40 GHz in the continuous-wave (CW) mode.

1 Experiments

The schematic cross section of MIS-HEMTs is shown in Fig. 1(a). The AlN/GaN heterostructures in this study were grown on semi-insulating SiC substrates by metal-organic chemical vapor deposition (MOCVD), consisting of a Fe-doped GaN buffer layer, an unintentionally doped GaN channel layer, 1 nm AlN spacer layer, a 5 nm AlN barrier layer, and 5 nm SiN_x insulator layer. Device fabrication was started with source/drain ohmic contact formation by Ti/Al/Ni/Au stack, and subsequent rapid thermal annealed at 800 ℃ for 30 s in N_2 atmosphere, to yield a contact resistance of 0.3 Ω·mm. Device isolation was then formed utilizing multiple-energy nitrogen ion implantation. A T-shaped gate was subsequently accomplished by electron beam lithography (EBL; model manufacturer) of UVIII/Al/PMMA resist stack. The width of the T-gate foot and head are 0.15 and 0.6 μm, respectively[2]. A Ni/Au metal layer was generated by e-beam evaporation (EVA450) on SiN_x's surface for the gate contact. Finally, the AlN/GaN HEMT devices were passivated with 60 nm stress-free SiN_x grown by plasma-enhanced chemical vapor deposition (PECVD). The fabricated MIS-HEMTs have a

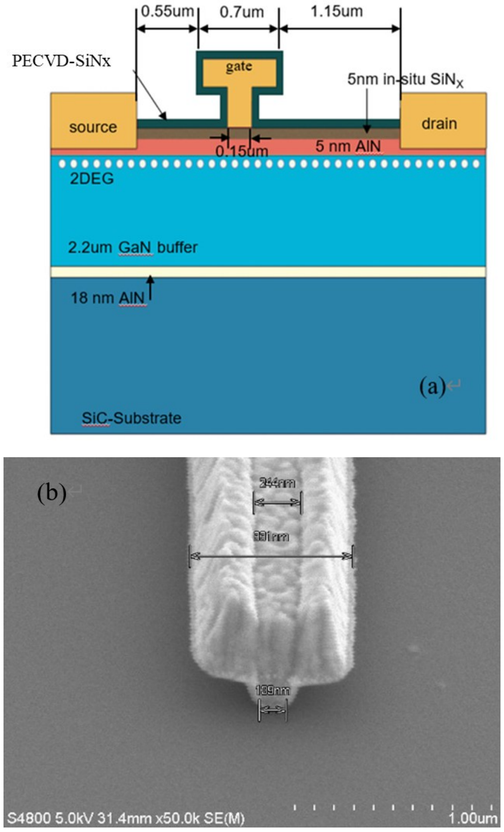

Fig.1 (a) The schematic of epitaxial structure of AlN/GaN MIS-HEMTs, (b) the SEM of 0.15-μm T-gate
图1 (a)外延材料与器件结构示意图,(b)0.15 μmT型栅扫描电镜图

source-drain distance (L_{SD}) of 2.4 μm and a gate-drain distance (L_{GD}) of 1.15 μm. An SEM picture of the T-gate is shown in Fig. 1(b).

As a comparison, AlGaN/GaN HEMT devices are also developed, with the barrier and cap layers replaced with a 21-nm $Al_{0.25}Ga_{0.75}N$ and a 3-nm GaN layers, respectively, as Ref. [16]. The gate recessed process, which differs from the AlN/GaN device's, uses inductively coupled plasma (ICP) dry etching with chlorine-based plasmas of BCl_3 and Cl_2 to fabricate recessed-gate with a width of 0.8 μm and depth of 6 nm. Then the same T-shaped gates were fabricated on it. The remaining process steps are the same as for AlN/GaN devices.

2 Results and discussions

2.1 DC measurement

The fabricated devices yielded in this study exhibit a typical static characterization, as shown in Fig. 2(a). Due to the much stronger spontaneous and piezoelectric polarization of AlN/GaN, a maximum drain current of

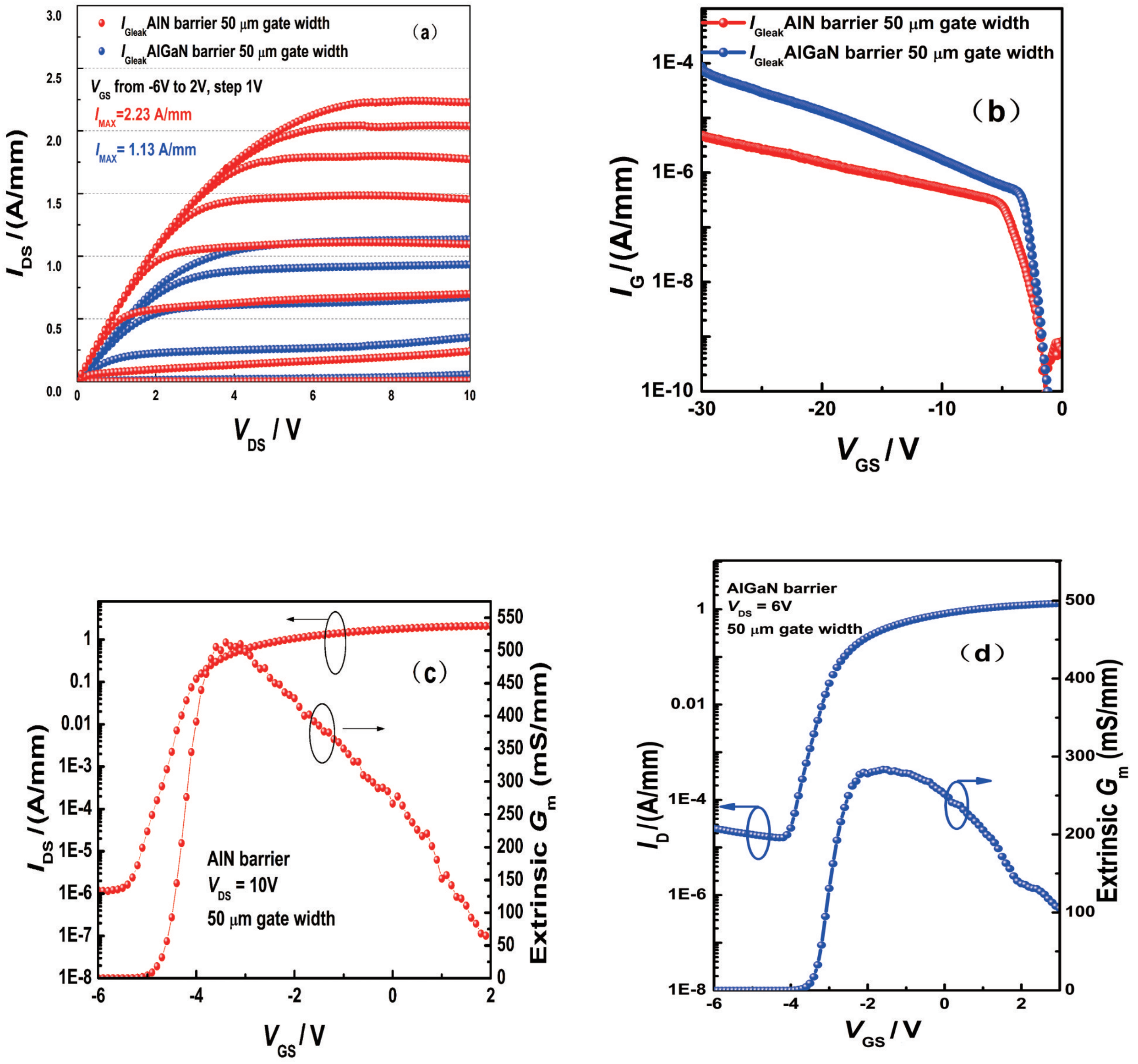

Fig. 2 Measured dc characteristics of devices (a) I_D of both HEMTs and MIS-HEMTs versus V_{DS} with V_{GS} varied from -6 V to 2 V, (b) gate leakage of HEMTs and MIS-HEMTs with V_{GS} swept to -30 V, (c) I_D and extrinsic transconductance of MIS-HEMTs with V_{GS} varied from -6 V to 2 V at V_{DS}= 6 V, (d) I_D and extrinsic transconductance of HEMTs with V_{GS} varied from -6 V to 3 V at V_{DS}= 6 V
图2 器件直流特性测试(a) HEMT 和 MIS-HEMT 器件输出电流特性测试对比图,(b) HEMT 和 MIS-HEMT 器件肖特基特性测试对比图,(c)MIS-HEMT 器件转移特性测试图,(d)HEMT 器件转移特性测试图

2.2 A/mm at V_{GS}=2 V was observed. The thickness of the in-situ SiN_x cap layer is critical for highly scaled GaN devices to avoid gate leakage current contributing to a reverse density of 4.7×10^{-6} A/mm at V_{GS} = -30 V, as shown in Fig. 2(b). The short-channel effect was effectively suppressed by the thin barrier, as shown by the transfer curves in Fig. 2(c), and the OFF-state drain leakage is merely 1.0×10^{-6} A/mm. Meanwhile the corresponding $G_{m,ext}$ at V_{DS} = 6 V is 509 mS/mm (Fig. 2(c)). Based on AlGaN barrier device, $G_{m,ext}$ is 294 mS/mm and the OFF-state drain leakage is 8.2×10^{-5} A/mm under the same test condition (Fig. 2(d)).

2.2 The small-signal RF characteristics

The small-signal RF characteristics of the fabricated MIS-HEMTs were measured using a network analyzer in a frequency range from 100 MHz to 40 GHz. Values of current-gain cutoff frequency f_T and unit-power-gain frequency f_{MAX}, as shown in Fig. 4, were determined by 20 dB/dec line extrapolated from the small-signal current gain |h21|and maximum stable gain (MSG). At V_{DS}=10 V, f_T and f_{MAX} are 98 GHz and 165 GHz, respectively (Fig. 3). It implies that in-situ SiN_x technology effectively suppresses the RF-G_m collapse in mm-wave AlN/GaN HEMTs.

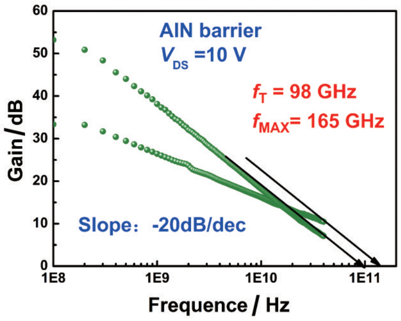

Fig. 3 Small-signal characteristics of the fabricated AlN/GaN MIS-HEMTs at V_{DS} = 10 V

图3 V_{DS} = 10 V下AlN/GaN MIS-HEMTs器件小信号测试图

2.3 CV and pulse measurement

To determine the quality of in-situ SiN_x, the capacitance-voltage (C-V) measurement was employed to realize interface trap density. The frequency/temperature dispersions of the second slope in C-V curve were analyzed[11-13], and the results are shown in Fig. 4. With f_m varying from 1 KHz to 1 MHz (Fig. 4(a)), and T increasing from 25 ℃ to 150 ℃ (Fig. 4(b)), the C-V characteristics of AlN/GaN MIS-HEMT exhibits a slight (ΔV less than 0.05 V) dispersions in multi-f/T ac-CV characteristics, indicating low Dit and high interface quality in MIS-HEMT. Accordingly, D_{it} at the in-situ SiN_x/AlN interface was mapped against E_T[14-15]. From E_C-0.58 eV to E_C -0.29 eV, D_{it} falls between 3.4×10^{11} and 1.1×10^{12} $cm^{-2}eV^{-1}$ (Fig. 4(c)).

The low interface state density ensures the low dc-RF dispersion, the pulse I-V characteristic of the devices is shown in Fig. 5(a). The pulse period and width were set to 10 μs and 200 ns, respectively. The gate-lag effect under a quiescent bias of (V_{GSQ}, V_{DSQ}) = (-6 V, 0 V) barely changes in the MIS-HEMTs. The drain-lag ratio under a quiescent bias of (V_{GSQ}, V_{DSQ}) = (-6 V, 15 V) is pretty weak in the saturation region (collapse ratio: 1.5%, Fig. 5(a)). It is probably due to the N in the SiN_x rather than the AlN barrier that leads N vacancies creating a conducting channel through the AlN barrier,

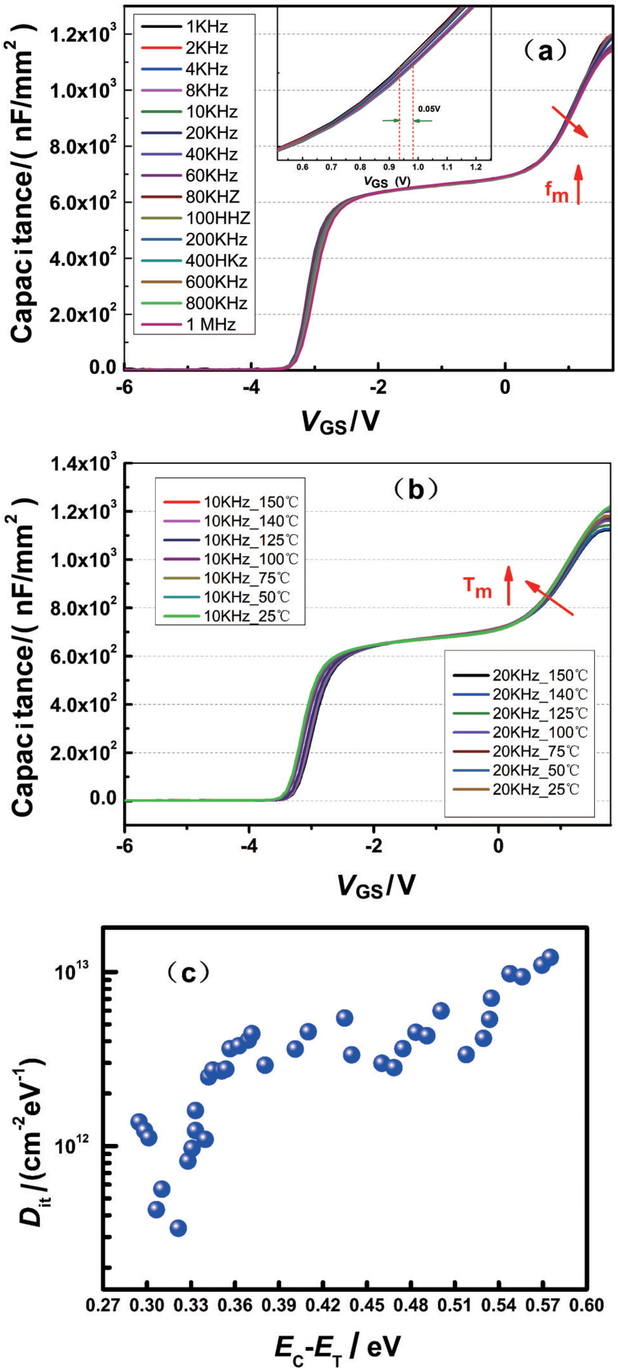

Fig. 4 f/T-dependent C-V characteristics of AlN/GaN MIS-HEMTs with (a) f_m varying from 1 KHz to 1 MHz, (b) T increasing from -25 °C to 150 °C f_m varying at 10 KHz and 20 KHz (c) D_{it}-E_T mapping in AlN/GaN MIS-HEMTs

图4 (a)AlN/GaN MIS-HEMTs不同频率下的CV测试图，(b)频率10 HKz和20 KHz下AlN/GaN MIS-HEMTs从-25到150 °C的CV特性测试图，(c)AlN/GaN MIS-HEMTs多频-变温下计算的D_{it}-E_T关系图

hence low annealing temperature and time. The in-situ $\mathrm{SiN_x}$ impeded the formation of nitrogen deficiency and oxidation of bare AlN surface when conventional process of ohmic annealing at above 800 °C, and suppressed damage to the AlN barrier during the process of extra $\mathrm{SiN_x}$ ex-situ passivation. The ultralow dispersion implies that in-situ $\mathrm{SiN_x}$ effectively obstructed the bombardment of ion when the plasm was generated. As shown the pulsed transfer characteristics curves in Fig. 5(b), hysteresis is less than 100 mV after sweeping from -8 V to 0 V, indicating significant suppression of deep interface traps with in-situ insulator.

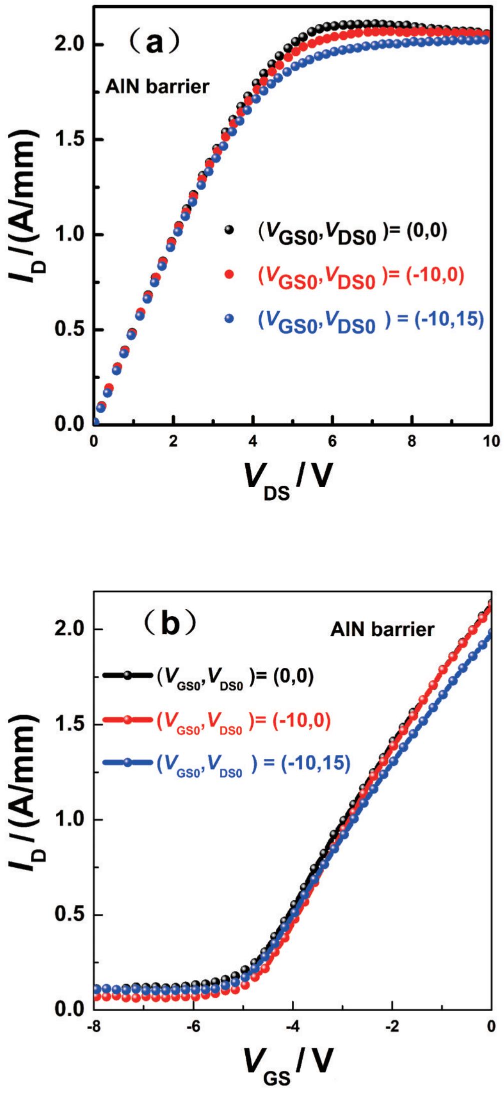

Fig. 5 Pulsed I-V characteristics of (a) output characteristics measured at V_{GS} = 0 V, (b) transfer characteristics measured at V_{DS} = 10 V

图5 脉冲测试图(a)V_{GS} = 0 V下,不同静态偏置下饱和输出电流测试对比图,(b)V_{DS} = 10 V时不同静态偏置下转移特性对比测试图

2.4 Large-signal measurement

Figure 6 depicts the large-signal power performance of the mm-wave AlN/GaN MIS-HEMTs, evaluated at 40 GHz in CW mode, in comparison with AlGaN/GaN HEMTs. The devices were biased at Class-AB condition with low operation voltage, V_{DS} = 8 V, V_{DS} = 10 V, and V_{DS} = 15 V, respectively. Load and source impedance were optimized for the best PAE before the evaluation.

Owing to the enlarged current density and minimized forward gate leakage current of AlN/GaN MIS-HEMTs, a record high PAE of 45.2% is achieved at V_{DS} = 8 V, and the corresponding output power density and associated gain are 2.3 W/mm and 10.8 dB gain. By contrast, the PAE, output power density, and gain of AlGaN/GaN HEMTs are merely 42.6%, 1.2 W/mm, and 9.1 dB respectively. when V_{DS} = 10 V, P_{out} of AlN/GaN MIS-HEMTs reached 3.3 W/mm while that of AlGaN/GaN HEMTs is 1.5 W/mm; when V_{DS} = 15 V, P_{out} of AlN/GaN MIS-HEMTs increased to 5.2 W/mm while that of AlGaN/GaN HEMTs is 2.8 W/mm. In previous research using the AlGaN HEMTs structure, P_{out} of 5.1 W/mm can be only obtained under V_{DS} over 25 V[16]. The high performance of AlN/GaN HEMTs is believed to attribute to the wide conduction band between AlN and GaN, as well as the high-quality $\mathrm{SiN_x}$/AlN interface.

At low voltage, the power density of AlN / GaN thin barrier MIS-HEMTs based on in-situ SiN growth is nearly double that of AlGaN barrier devices, making them promising for low voltage applications.

3 Conclusions

With in-situ $\mathrm{SiN_x}$ technique on AlN/GaN epi-structure and T-gate process, high-performance MIS-HEMTs have been fabricated for low V_{DS} applications at Ka-band. A high-quality $\mathrm{SiN_x}$/AlN interface has been obtained, which was verified by analyzing the frequency and temperature-dependent of the second slope in the C-V characteristics. Using 0.15 μm Γ-shaped gate technology, the developed MIS-HEMTs show a maximum drain current of 2.2 A/mm at V_{GS}=2 V, an extrinsic peak $G_{m,ext}$ of 509 mS/mm, extra-low dc-RF dispersion. The drain-lag ratio of 1.5% under a quiescent bias of (V_{GSQ}, V_{DSQ}) = (-6 V, 15 V) collapse-ratio in the saturation region. the MIS-HEMTs can yield an output power density of 2.3 W/mm associated with power-added efficiency (PAE) of 45.2% at 40 GHz under the drain voltage V_{DS}= 8 V in continuous-wave mode. Furthermore, when V_{DS}= 10 V, the power density was 3.3 W/mm, and PAE maintain 43.8%; when V_{DS}= 15 V, power density increased to 5.2 W/mm with PAE decreasing to 42.2%. The results suggest that the in-situ AlN/GaN MIS-HEMTs are promising for low bias voltage applications requiring high-efficiency and high-power density at Millimeter Waves.

References

[1] Moon J S. 55% PAE and high power Ka-band GaN HEMTs with linearized transconductance via n+ GaN source contact ledge[J]. *IEEE Electron Device Lett*, 2008, **29**(8): 834-7.

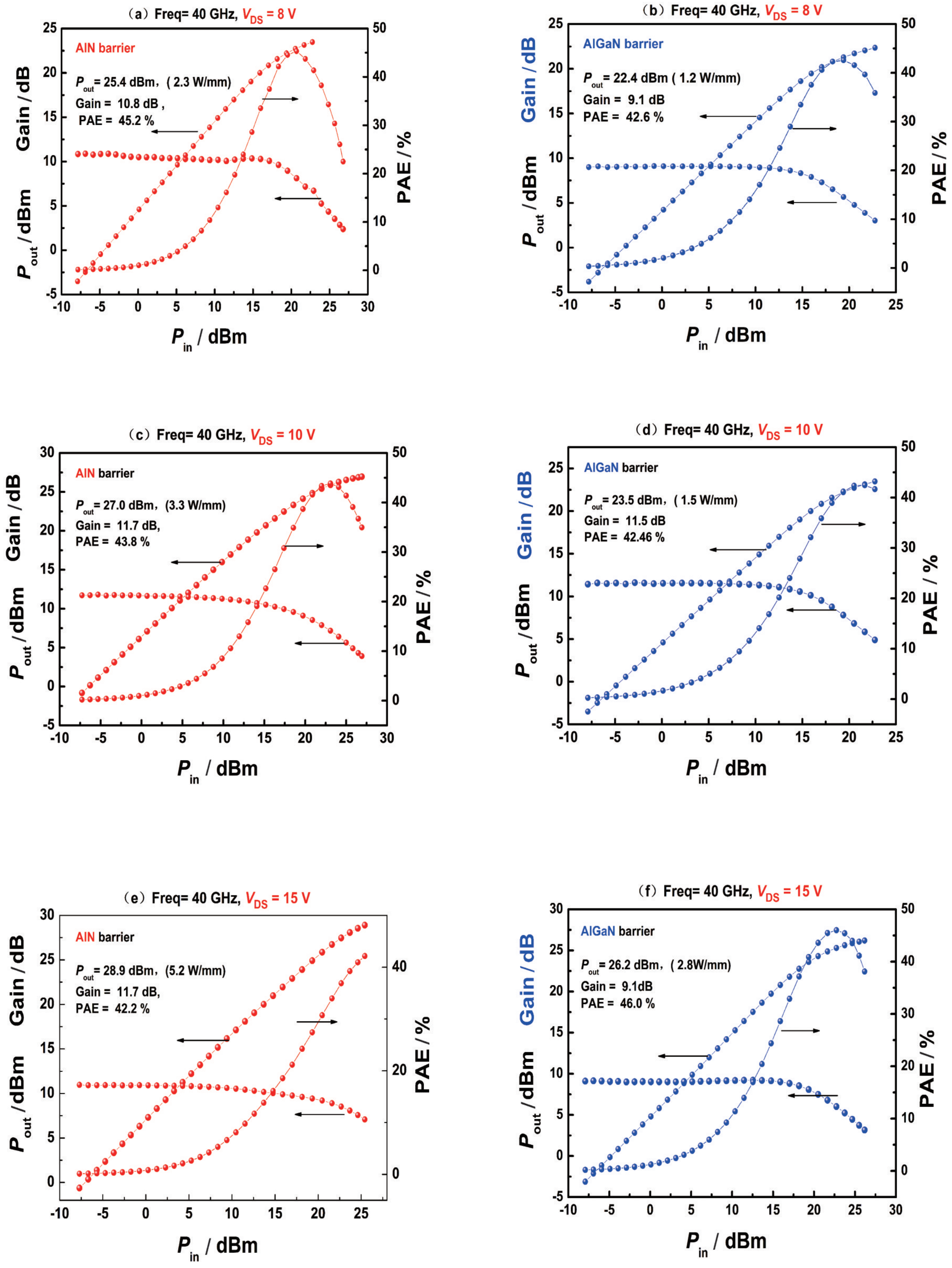

Fig. 6 Large-signal measurements at 40 GHz in CW mode (a) V_{DS}=8 V, AlN/GaN MIS-HEMTs measurement, (b) V_{DS}=8 V, AlGaN/GaN HEMTs measurement, (c) V_{DS}=10 V, AlN/GaN MIS-HEMTs measurement, (d) V_{DS}=10 V, AlGaN/GaN HEMTs measurement, (e) V_{DS}=15 V, AlN/GaN MIS-HEMTs large-signal measurement, (f) V_{DS}=15 V, AlGaN/GaN HEMTs measurement

图6 40 GHz下大信号连续波测试(a)V_{DS}=8 V, AlN/GaN MIS-HEMTs测试结果,(b)V_{DS}=8 V, AlGaN/GaN HEMTs测试结果,(c)V_{DS}=10 V, AlN/GaN MIS-HEMTs测试结果,(d)V_{DS}=8 V, AlGaN/GaN HEMTs测试结果,(e)V_{DS}=15 V, AlN/GaN MIS-HEMTs测试结果,(f)V_{DS}=15 V, AlGaN/GaN HEMTs测试结果

[2] Zhang Y C, Wei K, Huang S, *et al*. High-Temperature-Recessed Millimeter-Wave AlGaN/GaN HEMTs With 42.8% Power-Added-Efficiency at 35 GHz[J]. *IEEE Electron Device Letters*, 2018. **39** (5): 727-730.

[3] Downey B P, Meyer D J, Katzer D S, *et al*. Effect of SiNx gate insulator thickness on electrical properties of SiNx/In0.17Al0.83N/AlN/GaN MIS - HEMTs[J]. *Solid State Electronics*, 2015, 106(apr.): 12-17.

[4] Gu W P, Duan H T, Ni J Y, *et al*. High-electric-field-stress-induced degradation of SiN passivated AlGaN/GaN high electron mobility transistors SiN passivated AlGaN/GaN high electron mobility transistors [J]. *Chinese Physics B*, 2009, (4): 1601 -1608.

[5] Medjdoub F, Okada E, Grimbert B, *et al*. Towards millimeter-wave high PAE high power using ultrathin Al-rich barrier GaN devices. IEEE, 2015.

[6] Zimmermann, T, et al. AlN/GaN Insulated-Gate HEMTs With 2.3 A/mm Output Current and 480 mS/mm Transconductance [J]. *IEEE Electron Device Letters* 29.**7**(2008):661-664.

[7] Koehler A. D, Nepal N, *et al*. Atomic Layer Epitaxy AlN for Enhanced AlGaN/GaN HEMT Passivation [J]. *Electron Device Letters*, IEEE, 34.**9**(2013):1115-1117

[8] Hua M, Lu Y, Liu S, *et al*. Compatibility of AlN/SiNx Passivation With LPCVD-SiNx Gate Dielectric in GaN-Based MIS-HEMT[J]. *IEEE Electron Device Letters*, 2016, **37**(3):265-268.

[9] Taking S, Khokhar A, Macfarlane D, *et al*. New Process for Low Sheet and Ohmic Contact Resistance of AlN/GaN MOS-HEMTs[J]. 2010. European Microwave Week 2010: Connecting the World, EuMIC 2010 - Conference Proceedings (2010) **306**-309

[10] Al-Khalidi A, Khalid A, Wasige E. AlN/GaN HEMT technology with in-situ SiNx passivation[C]// 2015 11th Conference on Ph.D. Research in Microelectronics and Electronics (PRIME). IEEE, 2015. pp251-253

[11] Yang S , Tang Z, Wong K Y, *et al*. Mapping of interface traps in high-performance Al_2O_3/AlGaN/GaN MIS-heterostructures using frequency- and temperature-dependent C-V techniques[C]// IEEE International Electron Devices Meeting 2013. pp.631-634

[12] Yang S, Liu S, Lu Y, *et al*. Interface Trap Analysis in GaN-Based Buried-Channel MIS-HEMTs[J]. *IEEE Transactions on Electron Devices*, 2015, **62**(6):1870-1878.

[13] Mizue C, Hori Y, Miczek M, *et al*. Capacitance? Voltage Characteristics of Al2O3/AlGaN/GaN Structures and State Density Distribution at Al2O3/AlGaN Interface[J]. *Japanese Journal of Applied Physics*, 2011, **50**(2):021001-021001-7.

[14] M, Capriotti, P, et al. Modeling small-signal response of GaN-based metal-insulator-semiconductor high electron mobility transistor gate stack in spill-over regime: Effect of barrier resistance and interface states[J]. *Journal of Applied Physics*, 2015, **117**(2):24506-24506.

[15] Ramanan N, Lee B, Misra V. Comparison of Methods for Accurate Characterization of Interface Traps in GaN MOS-HFET Devices[J]. *IEEE Transactions on Electron Devices*, 2015, **62**(2):546-553.

[16] Zhang Y, Huang S, Wei K, *et al*. Millimeter-Wave AlGaN/GaN HEMTs with 43.6% Power-Added-Efficiency at 40 GHz Fabricated by Atomic Layer Etching Gate Recess[J]. *IEEE Electron Device Letters*, 2020, PP(99):1-1.